



ISSN: 0067-2904

Influence of Heat Transfer on MHD Oscillatory Flow for Eyring-Powell Fluid through a Porous Medium with Varying Temperature and Concentration

Dheia Gaze Salih Al –Khafajy*, Lqaa Tareq Hadi

Department of Mathematics, College of Science, University of Al-Qadisiyah, Diwaniya, Iraq

Received: 18/3/2020

Accepted: 8/6/2020

Abstract

The aim of this research is to study the effect of heat transfer on the oscillating flow of the hydrodynamics magnetizing Eyring-Powell fluid through a porous medium under the influence of temperature and concentration for two types of engineering conditions "Poiseuille flow and Couette flow". We used the perturbation method to obtain a clear formula for fluid motion. The results obtained are illustrated by graphs.

Keywords: Eyring-Powell fluid, MHD, Oscillatory flow, Porous medium.

تأثير انتقال الحرارة على التدفق التذبذبي للهيدروديناميكا الممغنطة لمائع (Eyring-Powell) خلال وسط مسامي مع تغير درجة الحرارة والتركيز

ضياء غازي صالح الخفاجي*, لقاء طارق هادي
قسم الرياضيات، كلية العلوم، جامعة القادسية، الديوانية، العراق

الخلاصة

الهدف من هذا البحث هو دراسة تأثير انتقال الحرارة على التدفق التذبذبي للهيدروديناميكا الممغنطة لمائع (Eyring-Powell) خلال وسط مسامي تحت تأثير درجة حرارة وتركيز لنوعين من التدفقات الهندسية (Poiseuille و Couette). استخدمنا طريقة الاضطراب للحصول على صيغة واضحة لحركة المائع. النتائج التي حصلنا عليها موضحة برسوم بيانية.

1. Introduction

Many researchers have been interested in the analysis of non-Newtonian fluids during the past few decades. The main concept behind MHD is that magnetic fields can stimulate currents in a moving conductive fluid which in turn polarizes the fluid and similarly changes the magnetic field itself. MHD plays an important role in different areas of science and technology. Nigamf and Singhj [1] studied the flow between parallel plates under the influence of the transverse magnetic field and heat transfer. Raptis *et al.* [2] studied the hydro-magnetic free convection flow through a porous medium between two parallel plates. Hamza *et al.* [3] discussed the effects of the slipping state as well as the transverse magnetic field and the radiative heat transfer for the unstable flow of a thin fluid. Khudair and Al-khafajy [4] discussed the effect of heat-transfer on MHD oscillatory flow for Williamson fluid through the porous medium. Migtaa and Al-khafajy discussed the effect of heat transfer on the MHD oscillatory flow of Carreau-Yasuda fluid through a porous medium [5]. Hayat and Abdulhadi [6] discussed the peristaltic transport of MHD Eyring-Powell fluid through porous medium in a three

*Email: dr.dheia.g.salih@gmail.com

dimensional rectangular duct. Hussain *et al.* analyzed the MHD flow of Powell-Eyring fluid by a stretching cylinder with Newtonian heating [7]. Begam and Deivanayaki studied the pulsatile flow of Eyring-powell nanofluid with Hall effect through a porous medium in [8]. More details about this topic are provided elsewhere [9-17].

Recently, a group of researchers described the effects of temperature and concentration on fluid movement. Most of these investigations agreed that the increase in temperature increases the velocity of the fluid while the fluid velocity changes in an unclear manner with the difference in concentration and according to the location of the fluid in the channel [16-21].

The present analysis aims to discuss the effects of heat transfer on the oscillating flow of the hydrodynamics of magnetizing Eyring-Power fluid through a porous medium under the influence of temperature and concentration for two types of engineering flows "Poiseuille flow and Couette flow". To our knowledge, this attempt has not yet been explored.

This paper consists of six sections; section 1, which is the introduction, provides a historical overview of the studies that dealt with this topic. Section 2 includes the form of the flow channel with the formulation of the governing equations with boundaries conditions and the formula of the Eyring-Powell fluid equation. In section 3, we review the dimensionless transformations to formulate the governing equations in a way that helps in solving them. Section 4 includes problem-solving and finding the formula for temperature, concentration, and velocity for the two types of engineering flows. In sections 5 and 6, we discuss the results through illustrated graphs and review the most important observations that we reached.

2. Mathematical Formulation

Let us consider the flow of an Eyring-Powell fluid in a porous medium of width h under the effects of the electrically applied magnetic field and radioactive heat transfer, as illustrated in Figure-1. Suppose that the fluid has very small electromagnetic force and the electrical conductivity is small. We are considering Cartesian coordinate system such that $(u(y), 0, 0)$ is a velocity vector in which u is the x -component of velocity and y is perpendicular to the x -axis.

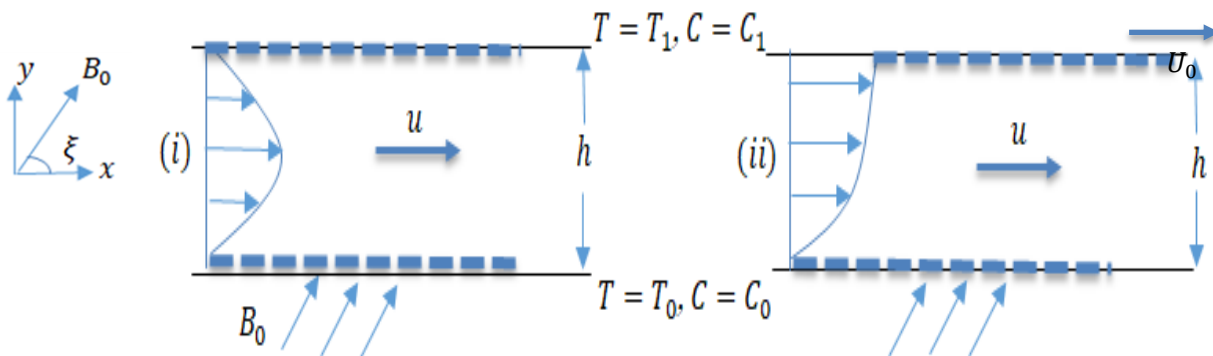


Figure 1 Channel format: (i) Poiseuille flow and (ii) Couette flow.

The basic equations governing Eyring – Powell fluid are given by:

The continuity equation is given by: $\frac{\partial \bar{u}}{\partial \bar{x}} + \frac{\partial \bar{v}}{\partial \bar{y}} = 0$. (1)

The momentum equations are:

In the x - direction: $\rho \left(\frac{\partial \bar{u}}{\partial \bar{t}} + \bar{u} \frac{\partial \bar{u}}{\partial \bar{x}} + \bar{v} \frac{\partial \bar{u}}{\partial \bar{y}} \right) = \frac{\partial \bar{S}_{xx}}{\partial \bar{x}} + \frac{\partial \bar{S}_{xy}}{\partial \bar{y}} + \rho g \beta_T (T - T_0) + \rho g \beta_C (C - C_0) - \sigma B_0^2 \sin^2(\xi) \bar{u} - \frac{\mu_0}{k} \bar{u}$. (2)

In the y - direction: $\rho \left(\frac{\partial \bar{v}}{\partial \bar{t}} + \bar{u} \frac{\partial \bar{v}}{\partial \bar{x}} + \bar{v} \frac{\partial \bar{v}}{\partial \bar{y}} \right) = \frac{\partial \bar{S}_{xy}}{\partial \bar{x}} + \frac{\partial \bar{S}_{yy}}{\partial \bar{y}} - \frac{\mu_0}{k} \bar{v}$. (3)

The temperature equation is given by: $\frac{\partial T}{\partial \bar{t}} = \frac{K}{\rho C_p} \frac{\partial^2 T}{\partial \bar{y}^2} - \frac{1}{\rho C_p} \frac{\partial q}{\partial \bar{y}} + \frac{Q_H}{\rho C_p} (T - T_0)$. (4)

The concentration equation is given by: $\frac{\partial C}{\partial \bar{t}} = D \frac{\partial^2 C}{\partial \bar{y}^2} - Kr^* (C - C_0) + \frac{DK_T}{T_m} \frac{\partial^2 T}{\partial \bar{y}^2}$. (5)

where \bar{u} is the axial velocity, ρ is the density of the fluid, p is the pressure, σ is the electrical conductivity, B_0 is the strength of the magnetic field, and g is the acceleration due to gravity. In the same equations, we can define T as a temperature, C_p is specific heat at constant pressure, q is the radiation heat flux, and K is thermal conductivity.

In addition, Q_H is heat generation, D is the coefficient of mass diffusivity, $(0 \leq \xi \leq \pi)$ is the angle between velocity field and magnetic field strength, and K_T is the thermal diffusion ratio.

The corresponding boundary conditions are given below:

$$\left. \begin{aligned} \bar{u} &= 0 \text{ at } \bar{y} = 0 \text{ and } \bar{u} = 0 \text{ at } \bar{y} = h \text{ (for Poiseuille flow)} \\ \bar{u} &= 0 \text{ at } \bar{y} = 0 \text{ and } \bar{u} = U_0 \text{ at } \bar{y} = h \text{ (for Couette flow)} \\ T &= T_0, C = C_0 \text{ at } \bar{y} = 0 \text{ and } T = T_1, C = C_1 \text{ at } \bar{y} = h \end{aligned} \right\} \quad (6)$$

$$\frac{\partial q}{\partial y} = 4\eta^2(T_0 - T), \quad (7)$$

where η is the radiation absorption.

The fundamental equation for Eyring – Powell fluid is given by:

$$S = -\bar{p}I + \tau,$$

$$\bar{\tau} = \mu_0 \nabla \bar{V} + \frac{1}{B_1} \sinh^{-1} \left(\frac{1}{A_1} \nabla \bar{V} \right),$$

where \bar{p} is the pressure, I is the unit tensor, $\bar{\tau}$ is the extra stress tensor, μ_0 is the zero shear rate viscosity, and $\nabla \bar{V}$ is the velocity gradient. We can write the component of extra stress tensor as follows:

$$\bar{\tau}_{xx} = \bar{\tau}_{yy} = \bar{\tau}_{yx} = 0, \quad \bar{\tau}_{xy} = \left(\mu_0 + \frac{1}{B_1 A_1} \right) \frac{\partial \bar{u}}{\partial y} - \frac{1}{6B_1(A_1)^3} \left(\frac{\partial \bar{u}}{\partial y} \right)^3. \quad (8)$$

3. Method of Solution

The non-dimensional governing equations are given by:

$$\left. \begin{aligned} x &= \frac{\bar{x}}{h}, y = \frac{\bar{y}}{h}, u = \frac{\bar{u}}{U}, p = \frac{\bar{p}h}{\mu_0 U}, Pe = \frac{\rho h U c_p}{K}, t = \frac{\bar{t}U}{h}, Kr = \frac{h Kr^*}{U} \\ R &= \frac{4\eta^2 h^2}{K}, \tau_{xy} = \frac{h}{\mu_0 U} \bar{\tau}_{xy}, \Phi = \frac{C-C_0}{C_1-C_0}, \theta = \frac{T-T_0}{T_1-T_0}, W_1 = \frac{1}{\mu_0 B_1 A_1} \\ A &= \frac{W_1}{6} \left(\frac{U}{h A_1} \right)^2, Re = \frac{\rho h U}{\mu_0}, Da = \frac{k}{h^2}, Gr = \frac{\rho g \beta_T h^2 (T_1 - T_0)}{\mu_0 U}, Q = \frac{Q_H h^2}{K} \\ M_2^2 &= \frac{\sigma B_0^2 h^2}{\mu_0} \sin^2(\xi), Sc = \frac{Uh}{D}, Sr = \frac{DK_T(T_1 - T_0)}{UT_m h (C_1 - C_0)}, Gc = \frac{\rho g \beta_C h^2 (C_1 - C_0)}{\mu_0 U} \end{aligned} \right\} \quad (9)$$

where U is the mean flow velocity, Da is the Darcy number, Re is the Reynolds number, M is the magnetic parameter, Pe is the Peclet number, R is the radiation parameter, Sc is the Schmidt number, Sr is the Soret number, Q is the heat generation parameter, T_m is the mean temperature, Gr is the thermal Grashof number, and Gc is the solutal Grashof number.

Substituting equations (7) - (9) into equations (1) - (6) yields the following nondimensional equations:

$$\frac{\partial u}{\partial x} + \frac{\partial v}{\partial y} = 0. \quad (10)$$

$$Re \frac{\partial u}{\partial t} = -\frac{dp}{dx} + \frac{\partial \tau_{xy}}{\partial y} + Gr\theta + Gc\Phi - \left(M_2^2 + \frac{1}{Da} \right) u. \quad (11)$$

$$\frac{\partial p}{\partial y} = 0. \quad (12)$$

$$Pe \frac{\partial \theta}{\partial t} = \frac{\partial^2 \theta}{\partial y^2} + (R + Q)\theta. \quad (13)$$

$$\frac{\partial \Phi}{\partial t} = \frac{1}{Sc} \frac{\partial^2 \Phi}{\partial y^2} - Kr\Phi + Sr \frac{\partial^2 \theta}{\partial y^2}. \quad (14)$$

where $M_2 = M \sin(\xi)$

$$\tau_{xy} = (1 + W_1) \frac{\partial u}{\partial y} - A \left(\frac{\partial u}{\partial y} \right)^3. \quad (15)$$

With the boundary conditions

$$u(0) = 0, \quad u(1) = 0 \quad \text{(for Poiseuille flow)} \quad (16)$$

$$u(0) = 0, \quad u(1) = U_0. \quad \text{(for Couette flow)} \quad (17)$$

$$\theta(0) = 0, \theta(1) = 1 \text{ and } \Phi(0) = 0, \Phi(1) = 1. \quad (18)$$

By Substituting equation (15) into equation (11) after simple algebra, we have:

$$3A \left(\frac{\partial u}{\partial y} \right)^2 \frac{\partial^2 u}{\partial y^2} - (1 + W_1) \frac{\partial^2 u}{\partial y^2} + \left(M_2^2 + \frac{1}{Da} \right) u + Re \frac{\partial u}{\partial t} = -\frac{dp}{dx} + Gr\theta + Gc\Phi. \quad (19)$$

4. Solution of the Problem

This section contains the solution to the governing equations that is related to the above equations.

4.1. Solution of the Heat and Concentration Equations

To achieve this solution, we use the separating variables method, by assuming that $\theta(y, t) =$

$e^{i\omega t}\theta_0(y)$ for heat equation (13) and $\Phi(y, t) = e^{i\omega t}\Phi_0(y)$ for the concentration equation (15), where ω is the frequency of oscillation with the boundary condition (18) [21]. As a result, we obtain the heat equation solution as follows:

$$\theta(y, t) = \csc(Z) \sin(Zy) e^{i\omega t}, \quad (20)$$

where $Z = \sqrt{R + Q - i\omega Pe}$.

The concentration equation solution is achieved by:

$$\Phi(y, t) = \left(\frac{e^{G(Z^2 + G^2 + Sr Sc Z^2)}}{(Z^2 + G^2)(e^{2G} - 1)} (e^{Gy} - e^{-Gy}) - \frac{Sr Sc Z^2 \csc[Z] \sin[Zy]}{Z^2 + G^2} \right) e^{i\omega t}, \quad (21)$$

where $G = \sqrt{Sc(Kr + i\omega)}$.

4.2. Solution of the Motion Equation

To solve the motion equation for two flows which are ‘‘Poiseuille flow and Couette flow’’, let

$$\frac{dp}{dx} = -\lambda e^{i\omega t}, \quad u(y, t) = u_1(y) e^{i\omega t}. \quad (22)$$

where λ is a real constant and ω is the frequency of the oscillation.

By substituting equation (22) into equation (19) then simplifying the result we get:

$$3Ae^{2i\omega t} \left(\frac{\partial u_1}{\partial y} \right)^2 \frac{\partial^2 u_1}{\partial y^2} - (1 + W_1) \frac{\partial^2 u_1}{\partial y^2} + \left(M_2^2 + \frac{1}{Da} \right) u_1 + i\omega Re u_1 = \lambda + Gr\theta_0 + Gc\Phi_0. \quad (23)$$

We assume a small value of A for the purpose of using the perturbation technique to solve the nonhomogeneous nonlinear partial differential equation (23). Accordingly, we write:

$$u_1 = u_{10} + Au_{11} + O(A^2). \quad (24)$$

Substituting equation (24) into equation (23) and applying boundary conditions, then equating the like powers of A , yields:

$$3Ae^{2i\omega t} \left(\frac{\partial}{\partial y} (u_{10} + Au_{11}) \right)^2 \frac{\partial^2}{\partial y^2} (u_{10} + Au_{11}) - (1 + W_1) \frac{\partial^2}{\partial y^2} (u_{10} + Au_{11}) + \left(M_2^2 + \frac{1}{Da} + i\omega Re \right) (u_{10} + Au_{11}) = \lambda + Gr\theta_0 + Gc\Phi_0. \quad (25)$$

4.2.1 Poiseuille flow

We employ the solution of equation (25) for Poiseuille flow by using boundary condition (16) to solve the zero and first orders system.

I - Zero-order system (A^0)

$$\frac{\partial^2 u_{10}}{\partial y^2} - \left(\frac{M_2^2 + \frac{1}{Da} + i\omega Re}{1 + W_1} \right) u_{10} = - \left(\frac{\lambda + Gr\theta_0 + Gc\Phi_0}{1 + W_1} \right).$$

with boundary conditions $u_{10}(0) = u_{10}(1) = 0$.

II - First-order system (A^1)

$$\frac{\partial^2 u_{11}}{\partial y^2} - \left(\frac{M_2^2 + \frac{1}{Da} + i\omega Re}{1 + W_1} \right) u_{11} = \frac{1}{1 + W_1} \left(3e^{2i\omega t} \frac{\partial^2 u_{10}}{\partial y^2} \left(\frac{\partial u_{10}}{\partial y} \right)^2 \right).$$

with boundary condition $u_{11}(0) = u_{11}(1) = 0$.

III - Zero-order solution

The solution of the zero-order equation subject to the associate boundary conditions is:

$$u_{10} = \frac{G}{\mathcal{F}} + e^{y\sqrt{\mathcal{F}}} \left(-\frac{G}{(1 + e^{\sqrt{\mathcal{F}}})\mathcal{F}} \right) + e^{-y\sqrt{\mathcal{F}}} \left(-\frac{e^{\sqrt{\mathcal{F}}}G}{(1 + e^{\sqrt{\mathcal{F}}})\mathcal{F}} \right).$$

III - First - order solution

The solution of the first-order equation subject to the associate boundary conditions is:

$$u_{11} = \frac{3e^{2i\omega t + \sqrt{\mathcal{F}} - y\sqrt{\mathcal{F}}} (1 + 2e^{\sqrt{\mathcal{F}}} + 2e^{2\sqrt{\mathcal{F}}} + e^{3\sqrt{\mathcal{F}}} + 4e^{\sqrt{\mathcal{F}}}\sqrt{\mathcal{F}}) \mathcal{G}^3}{8(1 + e^{\sqrt{\mathcal{F}}})^4 \mathcal{F}^2(1 + W_1)} + \frac{3e^{2i\omega t + y\sqrt{\mathcal{F}}} (1 + 2e^{\sqrt{\mathcal{F}}} + 2e^{2\sqrt{\mathcal{F}}} + e^{3\sqrt{\mathcal{F}}} - 4e^{2\sqrt{\mathcal{F}}}\sqrt{\mathcal{F}}) \mathcal{G}^3}{8(1 + e^{\sqrt{\mathcal{F}}})^4 \mathcal{F}^2(1 + W_1)} - \frac{(3e^{2i\omega t - 3y\sqrt{\mathcal{F}}} (2e^{(3-2y)\sqrt{\mathcal{F}}} + 2y\sqrt{\mathcal{F}}} + 2e^{2y\sqrt{\mathcal{F}} + (1+2y)\sqrt{\mathcal{F}}} - e^{3\sqrt{\mathcal{F}}} + e^{6y\sqrt{\mathcal{F}}} + 2e^{2(1+y)\sqrt{\mathcal{F}}} + 4e^{2\sqrt{\mathcal{F}} + 2y\sqrt{\mathcal{F}}} y\sqrt{\mathcal{F}} - 4e^{(1+4y)\sqrt{\mathcal{F}}} y\sqrt{\mathcal{F}}) \mathcal{G}^3)}{(8(1 + e^{\sqrt{\mathcal{F}}})^3 \mathcal{F}^2(1 + W_1))}$$

where $\mathcal{F} = ((M \text{Sin}[\xi])^2 + i\omega Re + \frac{1}{Da}) / (1 + W_1)$, $\mathcal{G} = ((\lambda + Gr\theta_0 + Gc\Phi_0) / (1 + W_1))$.

Hence, the fluid velocity is given by:

$$u(y, t) = (u_{10} + Au_{11}) e^{i\omega t}.$$

4.2.2 Couette flow

In this flow, the lower flake is fixed and the upper plate is moving with the velocity Uh . The

boundary conditions for the Couette flow problem are defined as:

$$(0)=0, (1)=U_0.$$

We simulate Couette flow by using the same previous method that we applied to solve Poiseuille flow in equation (25). The solution is calculated by the perturbation technique and the results are discussed with relevant figures.

5. Results and Discussion

We discuss the influence of heat transfer on MHD oscillatory flow for Eyring – Powell fluid through a porous medium with varying temperatures and concentrations for two types of engineering flows "Poiseuille flow and Couette flow" by using graphical illustrations. The temperature difference on both sides of the flow channel affects the fluid movement within the flow channel . The temperature difference depends on the parameters of R , Q , Pe and ω , as shown in the temperature charges. In equation (2) we notice the effects of different temperatures and concentrations, on both sides of the flow channel, on the fluid movement within the flow channel. We provide numerical assessments of analytical results and some of the graphically significant results that are presented in Figures- 2-23. We used the MATHEMATICA-12 program to find numerical results and illustrations. The velocity profile of the Poiseuille flow is shown in Figures- 2-9. Figure- 2 shows that velocity profile u decreases with increasing ω and W_1 . Figure-3 illustrates the influence of ξ and R on the velocity profiles u on the y axis. It is found that the velocity decreases with the increase of ξ while it increases with the increase of R . As illustrated in Figure-4, the velocity profile u increases with the increase of Gr and Gc , respectively, while it decreases with the increasing the parameters Sr and Sc , as shown in Figure-5. Figure-6 illustrates the influence of λ and Kr on the velocity profiles function u on the y axis. It is found that by increasing λ , the velocity increases, whereas it decreases with increasing Kr . We found that the velocity increases with increasing Da , Pe , Re and Q , as demonstrated in Figures-7 and 8, respectively. Figure-9 shows that the velocity increases with the increase of A and decreases with the increase of M . The velocity profile of Couette flow is shown in Figures- (10-17). It is found that the velocity increases with increasing the parameters R , Gr , Gc , λ , Da , Pe , Re , Q and A , respectively, while the velocity decreases with the increase of ω , W_1 , ξ , Sr , Sc , Kr and M . Based on equation (20), Figures- (18-19) show that the temperature increases with the increase in R , Q and Pe , while it decreases with the increase in ω . Based on equation (21), the concentration decreases with the increase of all parameters, (Figures- 20-23).

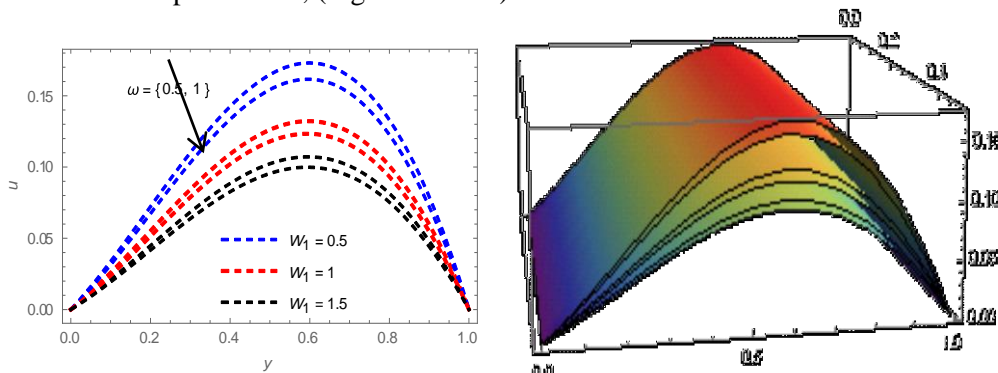


Figure 2-Poiseuille flow velocity profile for ω and W_1 with $A = 0.1, M = 1, Re = 2, Q = 2, Da = 0.8, \lambda = 1, Pe = 0.7, Sr = 0.2, Kr = 0.5, Sc = 0.6, Gr = 1, Gc = 1, \xi = \frac{\pi}{4}, t = 0.5, R = 2$.

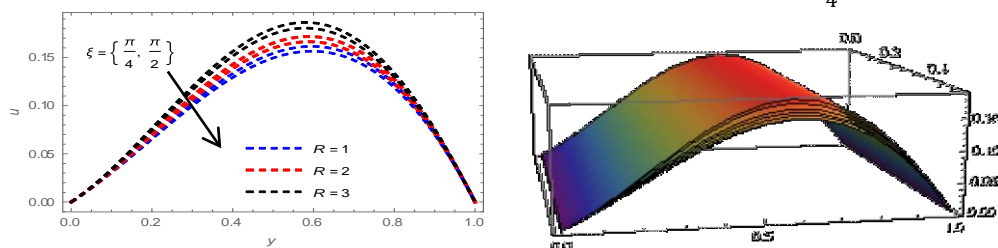


Figure 3-Poiseuille flow velocity profile for ξ and R with $\omega = 1, W_1 = 0.5, A = 0.1, M = 1, Re = 2, Q = 2, Da = 0.8, \lambda = 1, Pe = 0.7, Sr = 0.5, Kr = 0.5, Sc = 0.6, Gr = 1, Gc = 1, t = 0.5$.

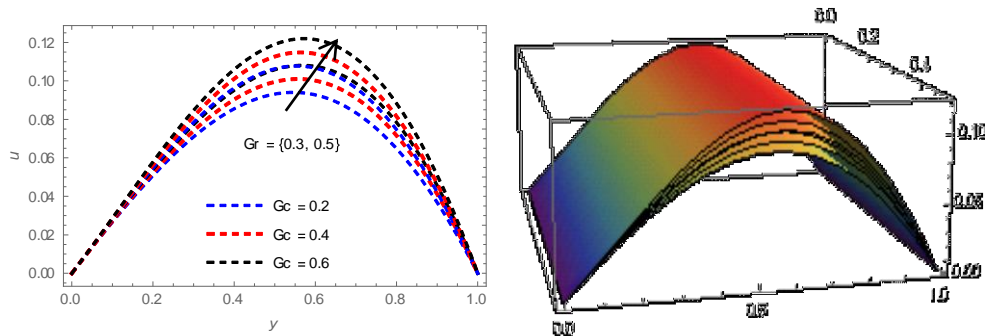


Figure 4-Poiseuille flow velocity profile for Gr and Gc with $\omega = 1, W_1 = 0.5, A = 0.1, M = 1, Re = 2, Q = 2, Da = 0.8, \lambda = 1, Pe = 0.7, Sr = 0.5, Kr = 0.5, Sc = 0.6, \xi = \frac{\pi}{4}, t = 0.5, R = 2.$

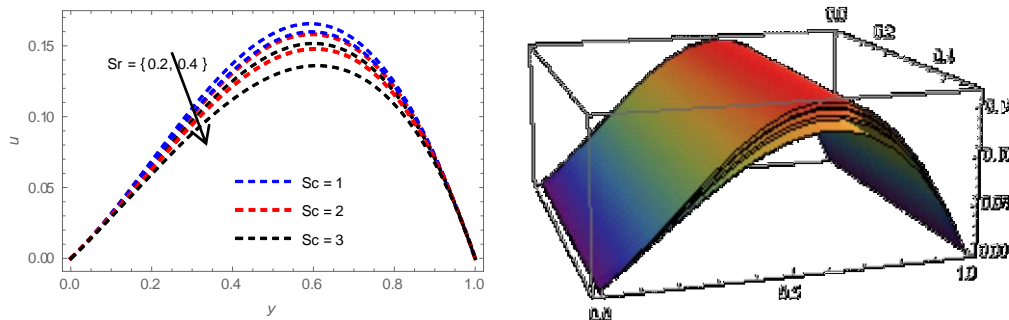


Figure 5-Poiseuille flow velocity profile for Sr and Sc with $\omega = 1, W_1 = 0.5, A = 0.1, M = 1, Re = 2, Q = 2, Da = 0.8, \lambda = 1, Pe = 0.7, Kr = 0.5, Gr = 1, Gc = 1, \xi = \frac{\pi}{4}, t = 0.5, R = 2.$

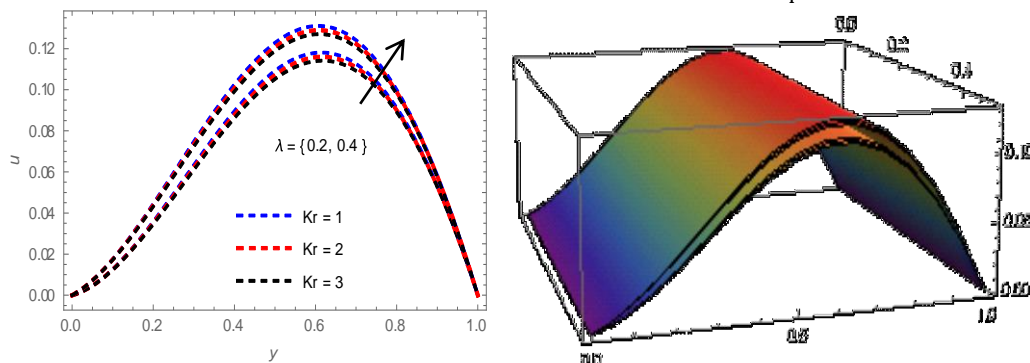


Figure 6-Poiseuille flow velocity profile for λ and Kr with $\omega = 1, W_1 = 0.5, A = 0.1, M = 1, Re = 2, Q = 2, Da = 0.8, Pe = 0.7, Sr = 0.5, Sc = 0.6, Gr = 1, Gc = 1, \xi = \frac{\pi}{4}, t = 0.5, R = 2.$

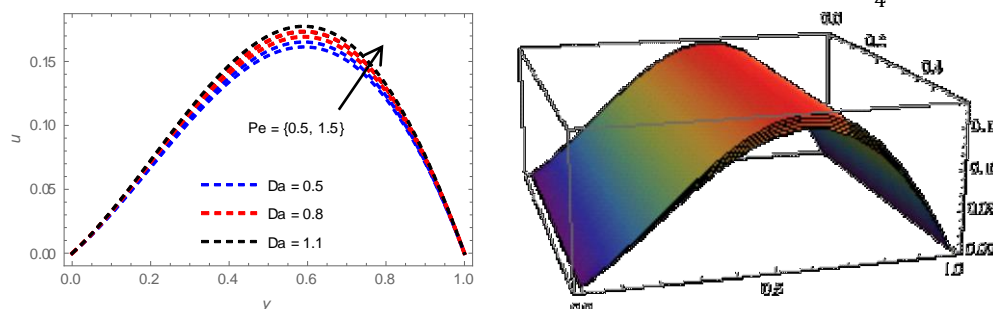


Figure 7-Poiseuille flow velocity profile for Da and Pe with $\omega = 1, W_1 = 0.5, A = 0.1, M = 1, Re = 2, Q = 2, \lambda = 1, Kr = 0.5, Sr = 0.5, Sc = 0.6, Gr = 1, Gc = 1, \xi = \frac{\pi}{4}, t = 0.5, R = 2.$

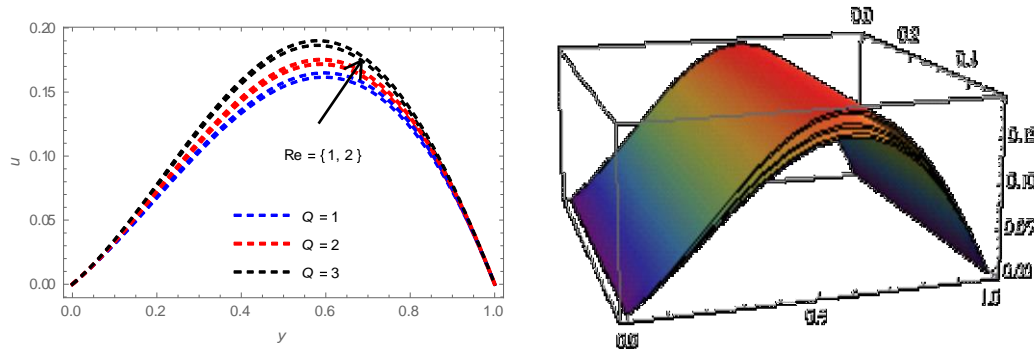


Figure 8-Poiseuille flow velocity profile for Re and Q with $\omega = 1, W_1 = 0.5, A = 0.1, M = 1, Da = 0.8, \lambda = 1, Pe = 0.7, Sr = 0.5, Sc = 0.6, Kr = 0.5, Gr = 1, Gc = 1, \xi = \frac{\pi}{4}, t = 0.5, R = 2$.

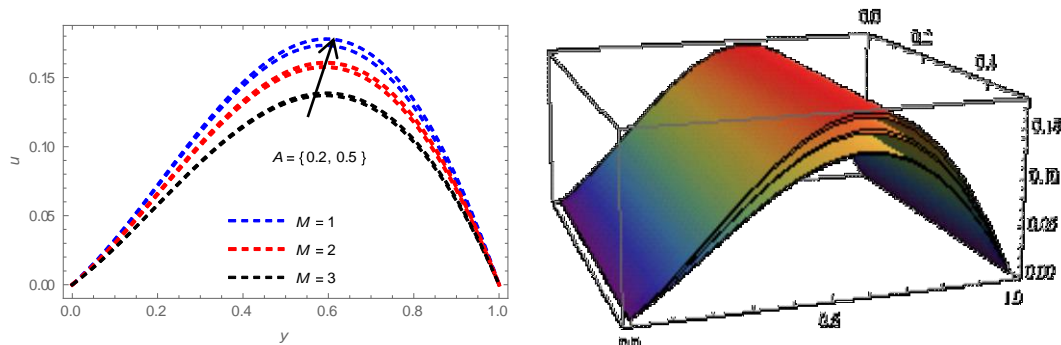


Figure 9-Poiseuille flow velocity profile for A and M with $\omega = 1, W_1 = 0.5, Re = 2, Q = 2, Da = 0.8, \lambda = 1, Pe = 0.7, Sr = 0.5, Sc = 0.6, Kr = 0.5, Gr = 1, Gc = 1, \xi = \frac{\pi}{4}, t = 0.5, R = 2$.

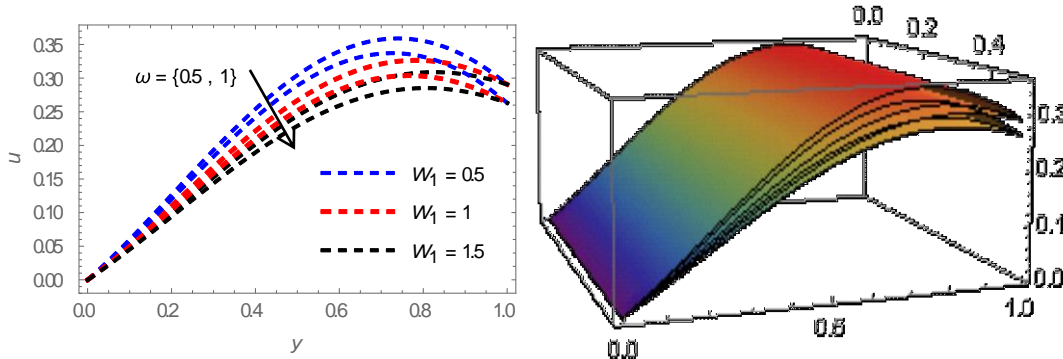


Figure 10-Couette flow velocity profile for ω and W_1 with $A = 0.1, M = 1, Re = 2, Q = 2, Da = 0.8, \lambda = 1, Pe = 0.7, Sr = 0.5, Kr = 0.5, Sc = 0.6, Gr = 1, Gc = 1, \xi = \frac{\pi}{4}, t = 0.5, R = 2$.

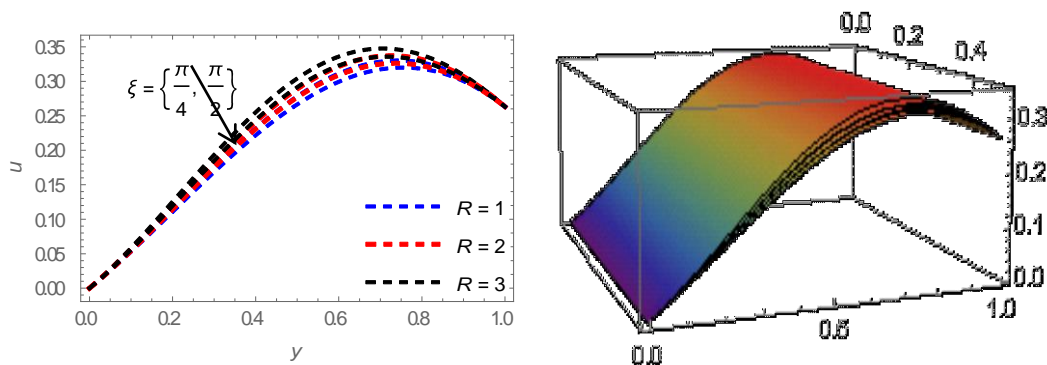


Figure 11-Couette flow velocity profile for ξ and R with $\omega = 1, W_1 = 0.5, A = 0.1, M = 1, Re = 2, Q = 2, Da = 0.8, \lambda = 1, Pe = 0.7, Sr = 0.5, Kr = 0.5, Sc = 0.6, Gr = 1, Gc = 1, t = 0.5$.

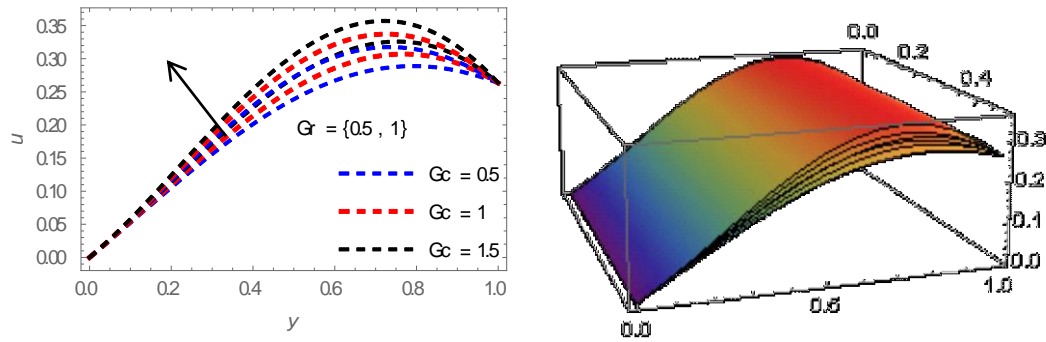


Figure 12-Couette flow velocity profile for Gr and Gc with $\omega = 1, W_1 = 0.5, A = 0.1, M = 1, Re = 2, Q = 2, Da = 0.8, \lambda = 1, Pe = 0.7, Sr = 0.5, Kr = 0.5, Sc = 0.6, \xi = \frac{\pi}{4}, t = 0.5, R = 2$.

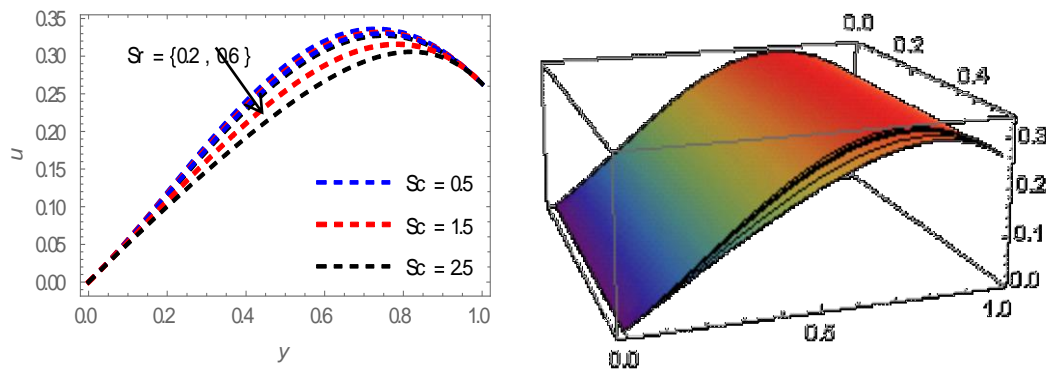


Figure 13-Couette flow velocity profile for Sr and Sc with $\omega = 1, W_1 = 0.5, A = 0.1, M = 1, Re = 2, Q = 2, Da = 0.8, \lambda = 1, Pe = 0.7, Kr = 0.5, Gr = 1, Gc = 1, \xi = \frac{\pi}{4}, t = 0.5, R = 2$.

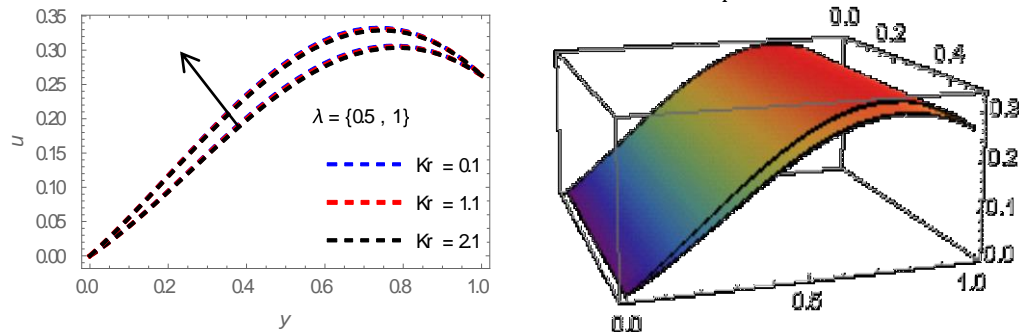


Figure 14-Couette flow velocity profile for λ and Kr with $\omega = 1, W_1 = 0.5, A = 0.1, M = 1, Re = 2, Q = 2, Da = 0.8, Pe = 0.7, Sr = 0.5, Sc = 0.6, Gr = 1, Gc = 1, \xi = \frac{\pi}{4}, t = 0.5, R = 2$.

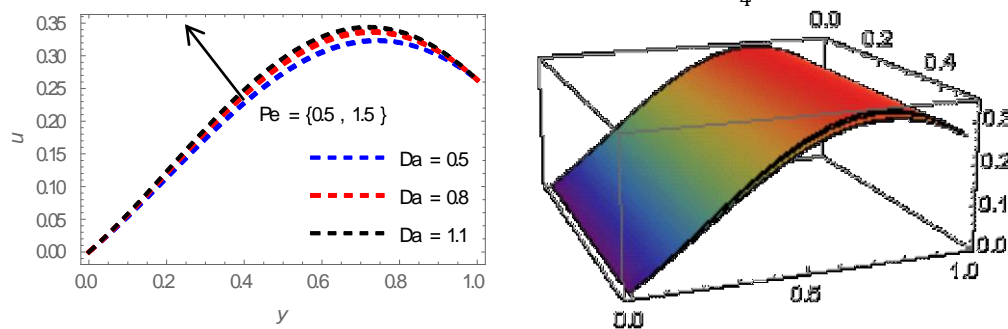


Figure 15-Couette flow velocity profile for Da and Pe with $\omega = 1, W_1 = 0.5, A = 0.1, M = 1, Re = 2, Q = 2, \lambda = 1, Kr = 0.5, Sr = 0.5, Sc = 0.6, Gr = 1, Gc = 1, \xi = \frac{\pi}{4}, t = 0.5, R = 2$.

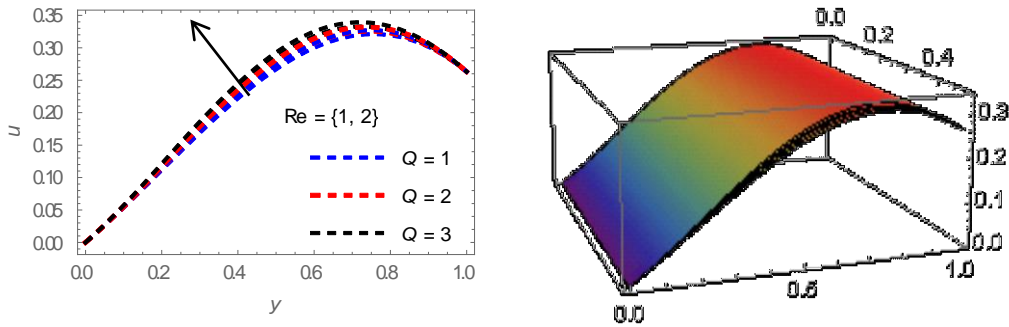


Figure 16-Couette flow velocity profile for Re and Q with $\omega = 1, W_1 = 0.5, A = 0.1, M = 1, Da = 0.8, \lambda = 1, Pe = 0.7, Sr = 0.5, Sc = 0.6, Kr = 0.5, Gr = 1, Gc = 1, \xi = \frac{\pi}{4}, t = 0.5, R = 2$.

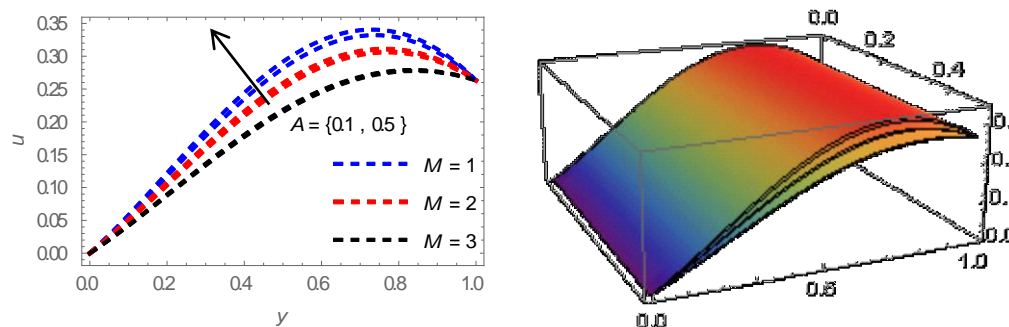


Figure 17-Couette flow velocity profile for A and M with $\omega = 1, W_1 = 0.5, Re = 2, Q = 2, Da = 0.8, \lambda = 1, Pe = 0.7, Sr = 0.1, Sc = 0.6, Kr = 0.5, Gr = 1, Gc = 1, \xi = \frac{\pi}{4}, t = 0.5, R = 2$.

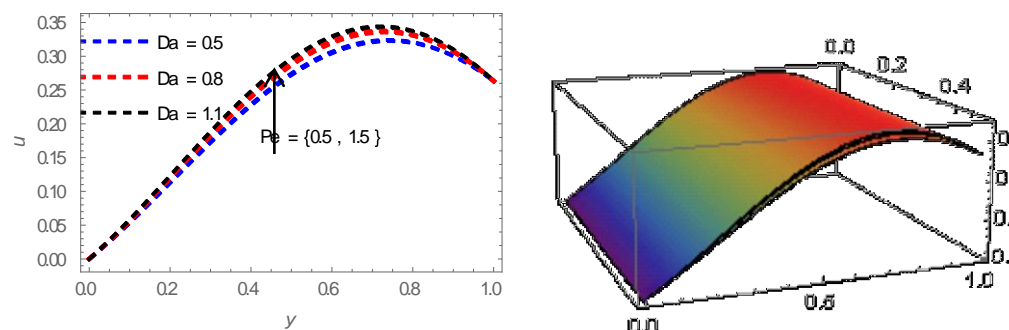


Figure 12-Couette flow velocity profile for Da and Pe with $\omega = 1, W_1 = 0.5, A = 0.1, M = 1, Re = 1, Q = 2, \lambda = 1, Kr = 0.5, Sr = 0.1, Sc = 0.6, Gr = 1, Gc = 1, \xi = \frac{\pi}{4}, U_0 = 0.3, t = 0.5, R = 2$.

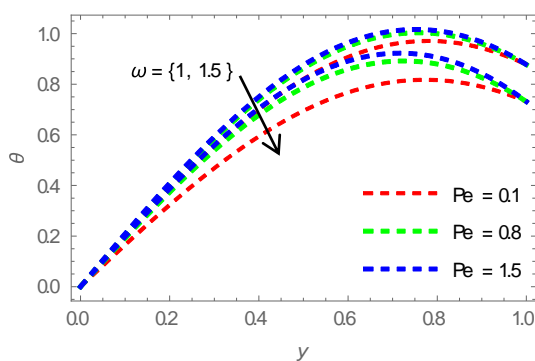


Figure 18 -Influence of ω and Pe on temperature θ for $R = 2, Q = 2, t = 0.5$.

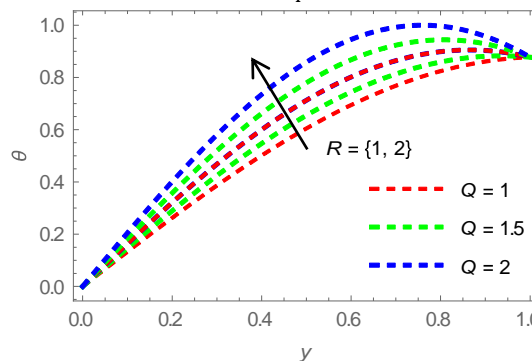


Figure 19-Influence of R and Q on temperature θ for $\omega = 1, Pe = 0.7, t = 0.5$.

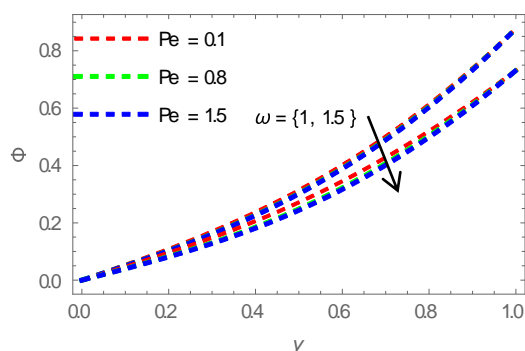


Figure 20-Influence of R and Q on concentration for $\omega = 1, Pe = 0.7$, $0.1, Kr = 0.5, Sc = 0.6, t = 0.5$.

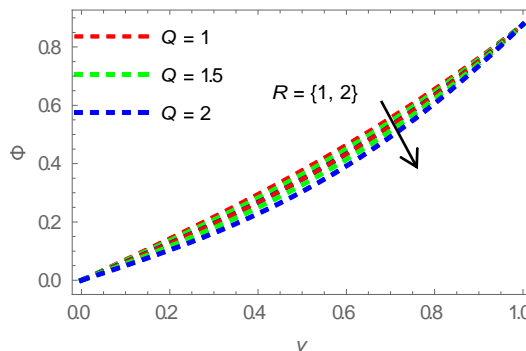


Figure 21 Influence of ω and Pe on concentration for $R = 2, Q = 2, Sr = 0.1$, $Sr = 0.1, Kr = 0.5, Sc = 0.6, t = 0.5$.

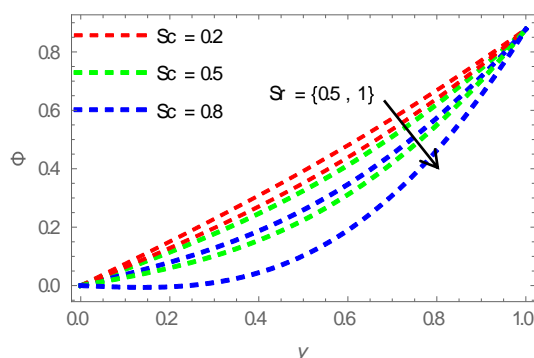


Figure 22-Influence of Sr and Sc on concentration for $\omega = 1, R = 2, Q = 2$, $Pe = 0.7, Kr = 0.5, t = 0.5$.

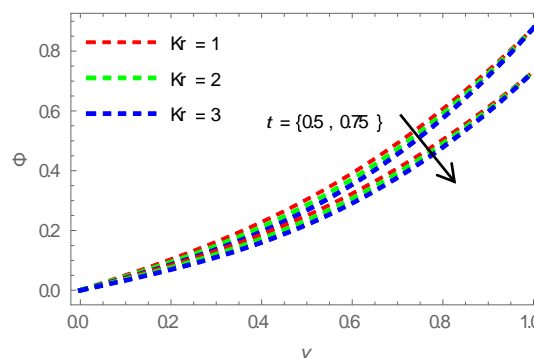


Figure 23-Influence of ω and Kr on concentration for $R = 2, Q = 2$, $Pe = 0.7, Sr = 0.1, Sc = 0.6, t = 0.5$.

6. Concluding Remarks

We discuss the influence of heat transfer on MHD oscillatory flow for Eyring-Powell fluid through a porous medium with varying temperature and concentration. Using the perturbation technique, we analyzed the velocity, temperature and concentration. We used different values to find the results of pertinent parameters, namely Darcy number, Peclet number, Grashof number, magnetic parameter, radiation parameter, Schmidt number, Soret number, heat generation parameter, frequency of the oscillation, and Reynold number. The key points are:

- In the two types of flow. i.e. Poiseuille and Couette, the velocity increases with increasing the parameters R , Gr , Gc , λ , Da , Pe , Re , Q and A , respectively, while the velocity decreases with increasing ω , W_1 , ξ , Sr , Sc , Kr and M .
- The temperature increases with the increase in R , Q and Pe while decreases with the increase in ω .
- The concentration decreases with the increase of all parameters.

References

1. B.S.D. Nigamf and S.N. Singhj. **1960**. Heat transfer by laminar flow between parallel plates under the action of transverse magnetic field, *Quart. Jour. Mech. Applied. Math*, **XIII**(5).
2. Raptis A., Massias C. and Tzivanidis G. **1982**. Hydromagnetic free convection flow during a porous medium between two parallel plates MHD, *Phys. Lett.*, **90A**: 288-289.
3. Hamza M. M., Isah B. Y. and Usman H. **2011**. Un-steady heat-transfer to MHD oscillatory flow during a porous medium under slip condition, *International Journal of Computer Applications*, **33**(4): 12-17.
4. W.S. Khudair and Dheia G.S. Al-khafajy. **2018**. Influence of heat-transfer on maneto-hydrodynamics oscillatory flow for Williamson fluid through a porous medium, *Iraqi Journal of science*, **59**(1B): 389-397.

5. H.A. Migtaa and Dheia G.S. Al-Khafajy. **2019**. Influence of heat transfer on magnetohydrodynamics oscillatory flow for Carreau-Yasuda fluid through a porous medium, *Journal of Al-Qadisiyah for computer science and mathematics*, **11**(3): 76-88.
6. Hayat A. Ali and Ahmed M. Abdulhadi. **2018**. The Peristaltic Transport of MHD Eyring-Powell Fluid through Porous Medium in a Three Dimensional Rectangular Duct, *International Journal of Pure and Applied Mathematics*, **119**(18).
7. Hayat Zakir Hussain, Muhammad Farooq and Ahmed Alsaedi. **2018**. Magnetohydrodynamics flow of Powell-Eyring fluid by a stretching cylinder with newtonian heating, *Thermal Science*, **22**(1B): 371-382.
8. M. Jannath Begam and M. Deivanayaki. **2019**. The Pulsatile Flow of Eyring-powell Nanofluid with Hall Effect through a Porous Medium, *Jour of Adv Research in Dynamical & Control Systems*, **11**(04).
9. Ray, A.K., Vasu, B., Murthy, P.V.S.N. **2020**. Non-similar Solution of Eyring–Powell Fluid Flow and Heat Transfer with Convective Boundary Condition: Homotopy Analysis Method. *Int. J. Appl. Comput. Math*, **6**(16). <https://doi.org/10.1007/s40819-019-0765-1>.
10. Gholinia, M., Hosseinzadeh, K., Mehrzadi, H., Ganji, D.D., Ranjbar, A.A. **2019**. Investigation of MHD Eyring-Powell fluid flow over a rotating disk under effect of homogeneous–heterogeneous reaction,. *Case Stud. Therm. Eng.* **13**: 100356.
11. Marwan A. Ahmed, Ahmed M. Abdulhadi, 2014, Influence of MHD for Newtonian Fluid and Heat Transfer in Microchannels between Two Parallel Plates Using HAM, *Iraqi Journal of science*, **55**(24): 537-547.
12. Ghadikolaie, S.S., Hosseinzadeh, K., Ganji, D.D., 2017, Analysis of unsteady MHD Eyring–Powell squeezing flow in stretching channel with considering thermal radiation and Joule heating effect using AGM, *Case Stud. Therm. Eng.* **10**: 579–594.
13. T.M. Agbaje, S. Mondal, S.S. Mosta, P. Sibanda, 2017, A numerical study of unsteady non-Newtonian Powell-Eyring nanofluid flow over a shrinking sheet with heat generation and thermal radiation, *Alexandria Engineering Journal*, **56**: 81–91.
14. Khalil-Ur-Rehman, M.Y. Malik, S. Bilal and M. Bibi. **2017**. Numerical analysis for MHD thermal and solutal stratified stagnation point flow of Eyring–Powell fluid induced by cylindrical surface with dual convection and heat generation effects, *Results in Physics*, **7**: 482-492.
15. Ramzan M., Bilal M. and Chung J.D. **2017**. Radiative Flow of Powell-Eyring Magneto-Nanofluid over a Stretching Cylinder with Chemical Reaction and Double Stratification near a Stagnation Point. *PLOS ONE*, **12**(1).
16. Wubshet Ibrahim. **2018**. Three dimensional rotating flow of Powell-Eyring nanofluid with non-Fourier's heat flux and non-Fick's mass flux theory, *Results in Physics*, **8**: 569–577.
17. Dheia G.S. Al-Khafajy. **2017**. Influence of MHD and Wall Properties on the Peristaltic Transport of a Williamson Fluid with Variable Viscosity Through Porous Medium, *Iraqi Journal of science*, **58**(2C): 1076-1089.
18. Iffat Jabeen, Muhammad Farooq and Nazir Ahmad Mir. **2019**. Description of stratification phenomena in the fluid reservoirs with first-order chemical reaction, *Advances in Mechanical Engineering*, **11**(4): 1–9.
19. Ahmed A.H. Al-Aridhee and Dheia G.S. Al-Khafajy. **2019**. Influence of MHD Peristaltic Transport for Jeffrey Fluid with Varying Temperature and Concentration through Porous Medium, *Journal of Physics: Conf. Series* 1294, 032012.
20. K. Javaherdeh, Mehrzad Mirzaei Nejad and M. Moslemi. **2015**. Natural convection heat and mass transfer in MHD fluid flow past a moving vertical plate with variable surface temperature and concentration in a medium, *Engineering Science and Technology, an International Journal*, **18**(3): 423-431.
21. Dheia G.S. Al-Khafajy. **2020**. Radiation and Mass Transfer Effects on MHD Oscillatory Flow for Carreau Fluid through an Inclined Porous Channel, *Iraqi Journal of science*, **61**(6).